Gulf General Atomic
Incorporated

GA-10280

FAST REACTOR SPECTRUM MEASUREMENTS

QUARTERLY PROGRESS REPORT
FOR THE PERIOD ENDING JULY 31, 1970

Prepared under
Contract AT(04-3)-167
Project Agreement No. 35
for the
San Francisco Operations Office
U. S. Atomic Energy Commission

August 24, 1970

LEGAL NOTICE

Gulf General Atomic
Incorporated
P.O. Box 608, San Diego, California 92112

GA-10280

FAST REACTOR SPECTRUM MEASUREMENTS

QUARTERLY PROGRESS REPORT
FOR THE PERIOD ENDING JULY 31, 1970

Work done by:

J. C. Young
G. M. Borgonovi
G. Bromley
P. d'Oultremont
P. R. Heid
D. H. Houston
C. H. Mirr
J. M. Neill
C. A. Preskitt
A. E. Profio
C. Rindfleisch

Report written by:

J. C. Young
P. d'Oultremont
G. M. Borgonovi
C. Rindfleisch
A. E. Profio

Prepared under
Contract AT(04-3)-167
Project Agreement No. 35
for the
San Francisco Operations Office
U. S. Atomic Energy Commission

Gulf General Atomic Project 4008

August 24, 1970

TABLE OF CONTENTS

LIST OF FIGURES

1. INTRODUCTION

This quarterly progress report describes the work performed during the period May 1, 1970 to July 31, 1970, on the program of Fast Reactor Spectrum Measurements under Contract AT(04-3)-167, Project Agreement No. 35 with the U. S. Atomic Energy Commission. Previous reports under this program are listed in Refs. 1 through 7.

During this quarter the main effort was directed towards the following:

1. Correction to STSF-1A analysis
2. Loading of STSF-7
3. Calculations for STSF-7
4. Cell calculation studies
5. Proton Recoil Detector Studies
6. He^3 neutron spectrometer studies
7. Time dependent ANISN code.

An improved data reduction for STSF-1A was made which modified the lower energy region of the neutron spectrum in this core. This new data reduction is described in Section 2. The agreement between the measured and calculated spectrum has improved but the general conclusions drawn previously are not changed.

The STSF-7 core was loaded during this quarter. Reactivity calculations to verify the subcriticality of the system have been performed as well as the calculations necessary for comparison to the time-of-flight data.

Some of the difficulties encountered in making cell calculations typical of fast reactors have been studied and are discussed in Section 5.

Proton recoil response functions have been measured for cylindrical hydrogen and methane detectors by time of flight. These detectors were also used to measure the neutron spectra in the core and the reflector of STSF-7.

The time-dependent transport code ANISN has been obtained and has been converted for use on the UNIVAC 1108 computer. Test problems* have been run using this code and the results are reported in Section 8. The preliminary results are promising but further tests need to be undertaken.

*We would like to acknowledge the assistance of B. Zolotar of ANL for obtaining these test problems for us.

2. STSF-1A NEUTRON SPECTRUM

As reported previously,[1] the neutron spectrum measured by time of flight in the core of the assembly STSF-1A (similar to ZPR-3, Assembly 57[8]) has been reduced and compared to transport calculation results. Subsequently it was found that the thickness of the boron filter placed in the flight path to prevent neutron burst overlapping was inadvertently taken as 0.3175 cm in the data reduction instead of the true value of 0.24 cm. The data has therefore been reduced again using the correct filter thickness and the results are shown in Figs. 1 and 2. The multigroup transport calculation results plotted on these two graphs are the same as reported in Ref. 1. As can be seen from Fig. 1 the agreement between the calculation and corrected experiment is better below ~ 5 keV neutron energy. However, the general trend remains the same.

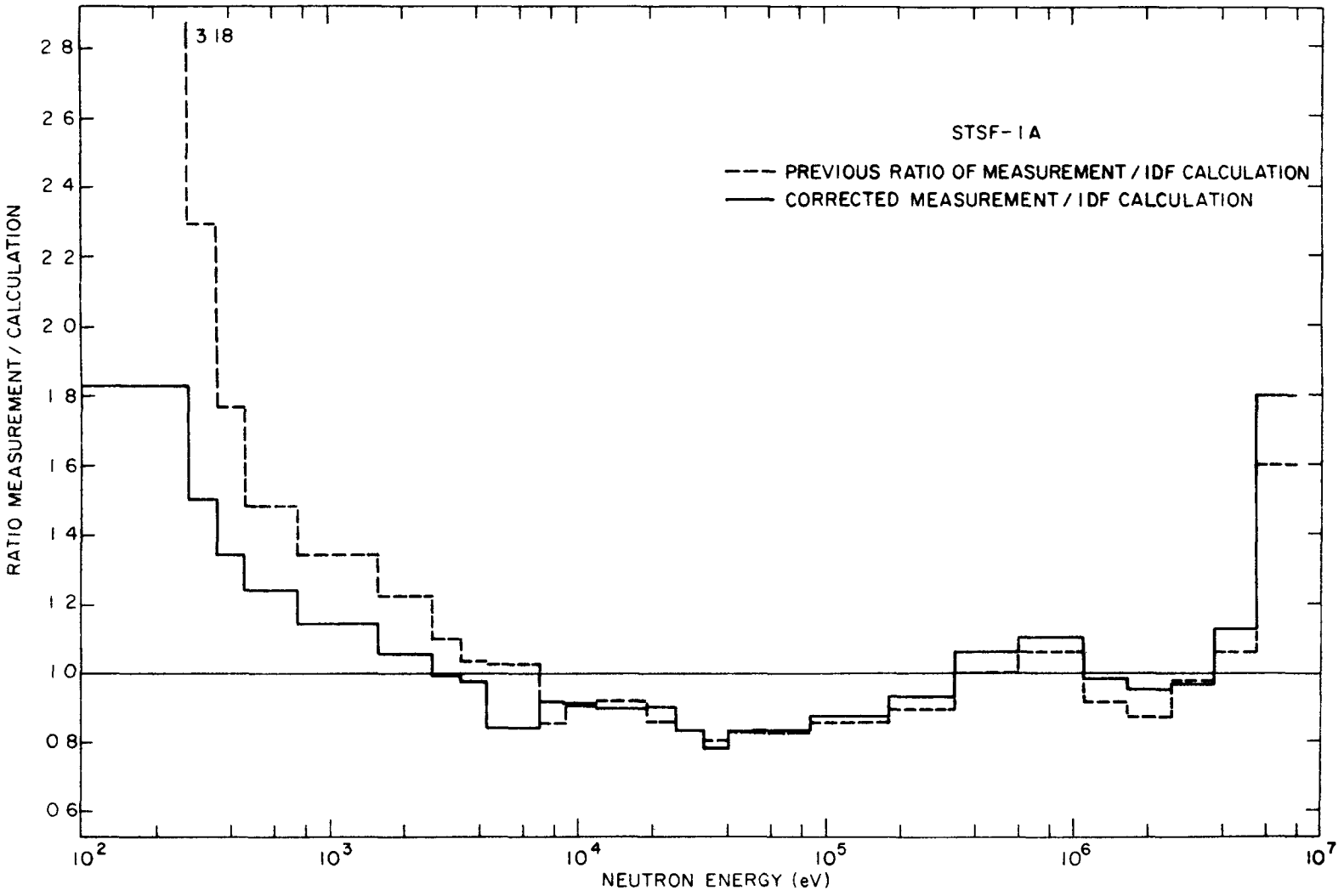

Fig. 1. Ratio of measurement to 1DF calculation for STSF-1A

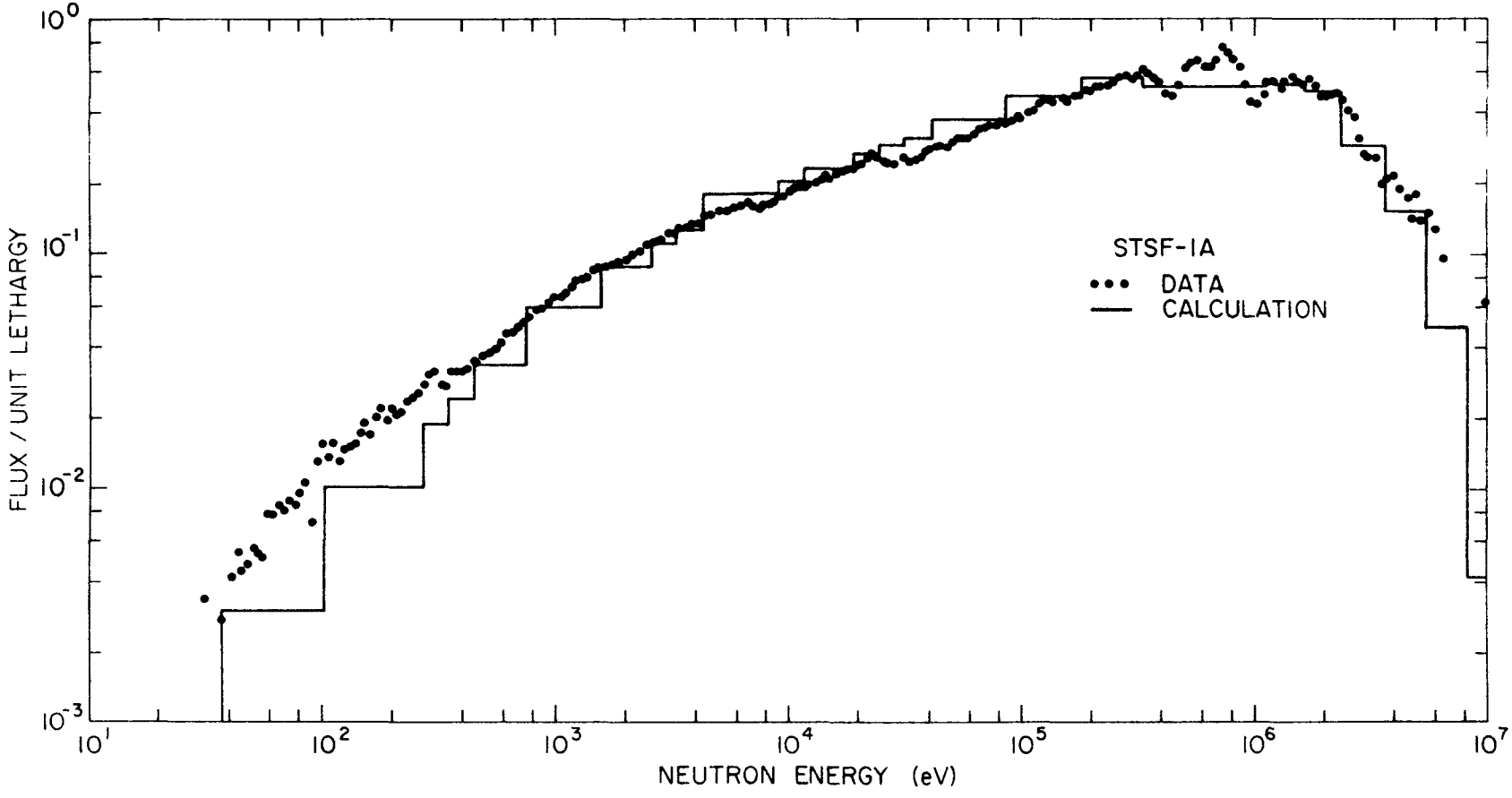

Fig. 2. Comparison of experimental data and 1DF calculation

3. STSF-7 CORE DESCRIPTION AND LOADING

The STSF-7 core is a $^{235}U/^{238}U$ system identical to ZPR-3 Assembly 11[8] except that, (1) the ZPR assembly had a steel matrix whereas STSF-7 has an aluminum matrix, and (2) the half-height of STSF-7 is 9 inches whereas that for ZPR is 10 inches. Table 1 gives the homogenized atom densities for both STSF-7 and the ZPR assembly.

Originally, the proposed loading for STSF-7 was 108.7 kg of ^{235}U which gave a symetrical geometry that could be easily represented in the calculations. However, the inverse multiplication curves obtained during loading, as well as the transport calculations, (Section 4), indicated that the above mass of ^{235}U would be much less than the desired \$10 subcritical. Therefore, we added additional fuel to bring us to the \$10 subcritical level and to the next best symmetrical configuration. This gave us a total loading of 144.5 kg of ^{235}U compared to a measured critical value of 240.6 kg of ^{235}U for ZPR-3 Assembly 11. The radial geometry of the movable half of the assembly for the configuration of the final loading of STSF-7 is shown in Fig. 3. This configuration consisted of 57 drawers loaded in the movable half of the assembly and 56 drawers in the fixed half.* Each drawer contained 1.279 kg of ^{235}U and the $^{235}U/^{238}U$ plates (1/8 x 2 x 3 inches) were arranged in the drawers as shown in Fig. 4.

*The fixed half has one less drawer to accommodate the Linac source.

Table 1

ATOM DENSITIES FOR STSF-7 AND ZPR-3 ASSEMBLY 11[9]

	STSF-7 (atoms/barn-cm)[a]		ZPR-3, Assembly 11 (atoms/barn-cm)	
Element	Core	Reflector	Core	Reflector
^{235}U	0.00466	0.00008	0.004567	0.000089
^{238}U	0.03616	0.03977	0.034392	0.040025
^{234}U			0.000046	
Fe			0.005681	0.004925
Cr			0.001486	0.001196
Ni			0.000718	0.000536
Mn			0.000208	
Al	0.00564	0.00564		0.000111

[a]The slight difference between the number densities reported for ZPR-3, Assembly 11 and the number densities for STSF-7 are believed to be due to differences in voids in the two systems. For convenience, our comparative calculations for the ANL assembly (Section 4) have utilized the fuel number densities for STSF-7.

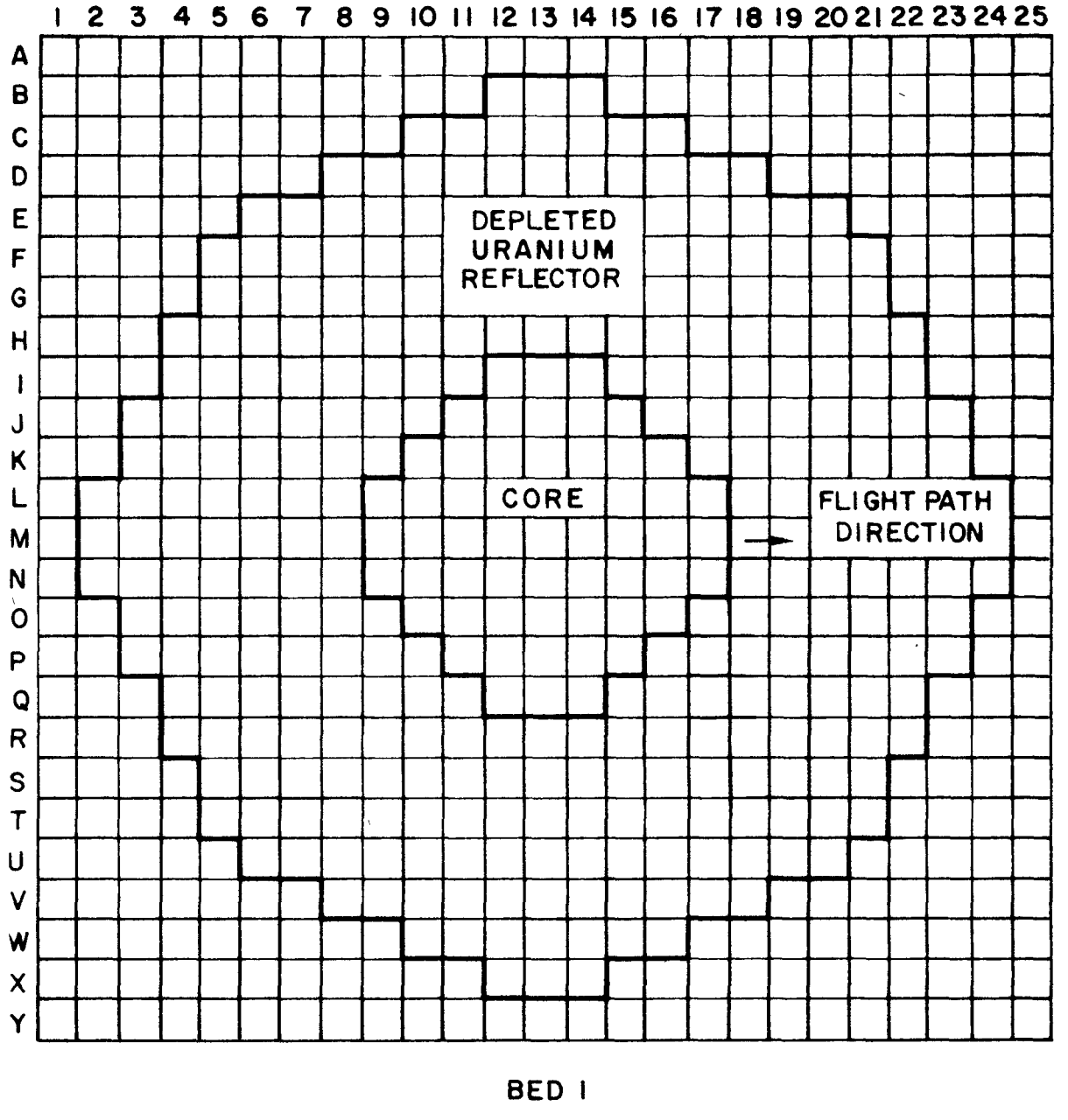

Fig. 3. Radial geometry for STSF-7

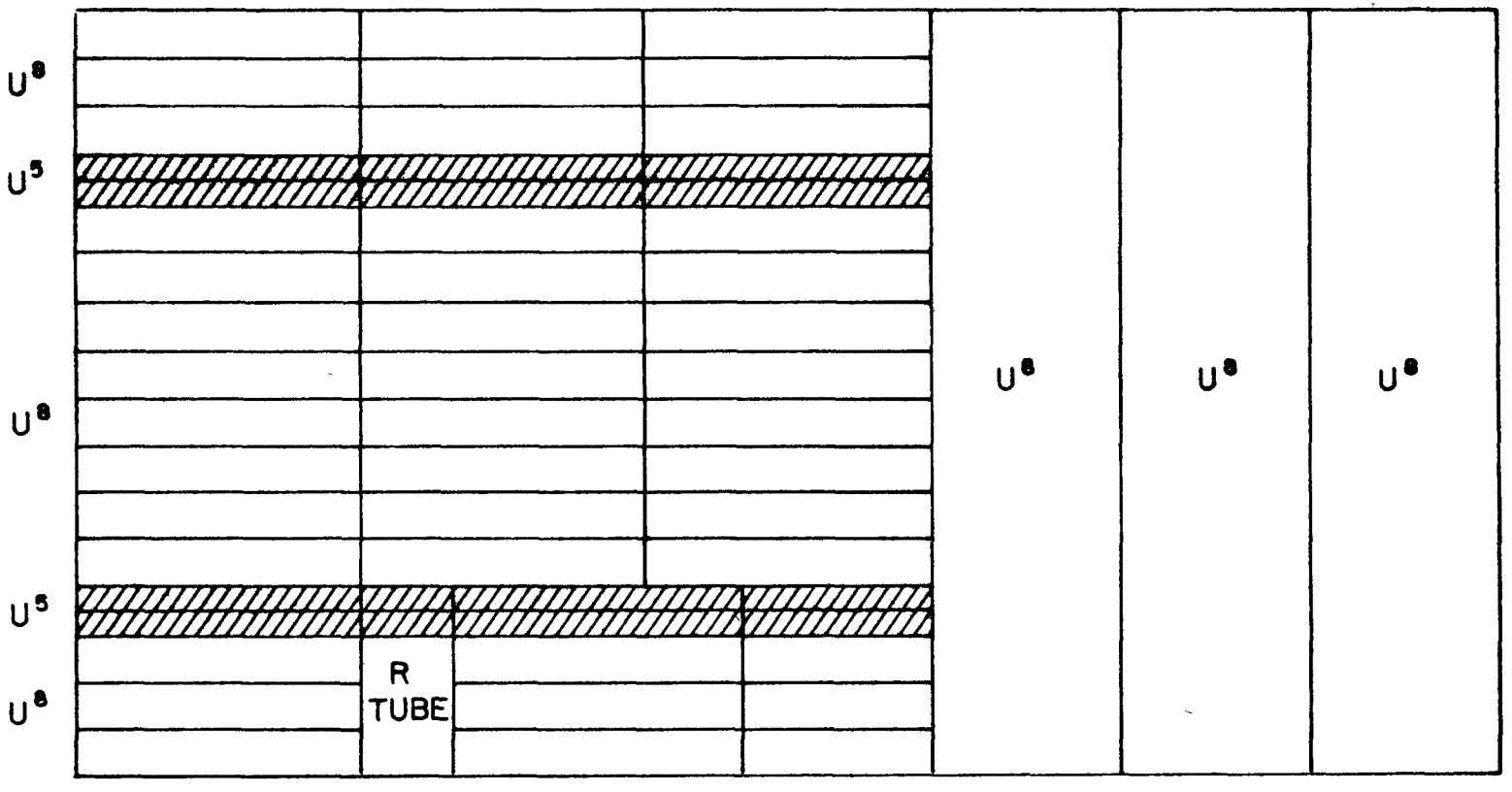

Fig. 4. Typical fuel drawer used in STSF-7

4. CRITICAL MASS AND SPECTRUM CALCULATIONS FOR STSF-7

Neutron transport calculations of STSF-7 have been made with the same methods employed for previous STSF assemblies[2] and using ENDF/B version 1 cross sections. It is, however, planned to recalculate the assembly with ENDF/B version 2 data in the near future. Let us briefly recall the sequences of calculation:

1. The GAM code[10] generates cross sections for the core spectrum components (Al, ^{235}U, ^{238}U) averaged over a spectrum obtained with the B-3 approximation and a buckling of 5×10^{-3} cm^2.
2. The transport code 1DF[11] performs an S_{16}, k calculation of the unit core cell. This provides disadvantage factors for the different plates of the cell that are used in the next calculation as self-shielding factors.
3. A second GAM run generates a set of cross sections for the homogenized core which takes into account the self-shielding due to the plate configuration of the cell.
4. 1DF is then used for spherical k and Q calculations of the whole system with S_4 or S_{16} quadrature according to the desired accuracy for the angular fluxes.

Some additional details will now be given concerning the critical mass evaluation and the determination of the cell heterogeneity.

4.1 THE STSF-7 k CALCULATION

The reactor has been loaded with 113 fuel drawers to give a core 45.75 cm long and 23.45 cm in radius with an L/D ratio of 0.976. This is an equivalent radius corresponding to the actual core cross sectional area.

The core volume is 78850 cm^3; this corresponds to a sphere 26.64 cm in radius. Using Davey's[12] recommendations, the shape factor for this case is 0.955; therefore, the sphere equivalent to the loaded core will have a volume of 0.955 x 78850 cm^3 or 75302 cm^3 and a radius of 26.2 cm. A 1DF S_4 k calculation of this sphere gives a k effective of 0.9143.

Now we wished to check our calculations by comparison to the critical ZPR-3, Assembly 11 which had a stainless steel structure. A second set of cross sections was therefore generated for the homogeneous core in which aluminum was replaced by steel. For the experimental critical mass of 240.6 kg of ^{235}U in the above assembly and a radius of 31.6 cm (obtained by using the appropriate shape factor), we calculated k effective to be 0.9866. This is in reasonable agreement with the value of 0.974 obtained with the same ENDF/B cross sections by Zolotar et. al.[13]

In order to be able to estimate the reactivity change due to the use of aluminum instead of steel in the core, the system k effective has been calculated in both cases for an arbitrary radius R of 30 cm. The results are k_{eff} (Al) = 0.9688 and k_{eff}(SST) = 0.9668 or a positive δk of $\sim$0.2% for the aluminum.

Since the k effective of the steel structured reactor was calculated for radii of 30 and 31.6 cm, it was possible to compute the edge drawer reactivity worth in the following manner:

Difference in k_{eff} (δk) = 1.9768×10^{-2} ,

Difference in mass (δ M-kg) = 34.78 kg ,

Taking β_{eff} as 7.4×10^{-3}, and since $\delta\rho = \frac{\delta k}{\beta k}$ (dollars) ,

Where $k = 1 - \frac{\delta k}{2}$,

we find that \$1 reactivity corresponds to 12.59 kg of ^{235}U. This is in good agreement with the experimental value[14] of 10 cents for an edge drawer which contains 1.28 kg ^{235}U.

4.2 CELL AND HETEROGENEITY CALCULATIONS

Since the beginning of this program, several ways of calculating the cell heterogeneity and of comparing the measured and calculated fine spatial structure of the flux have been investigated. The central difficulty has been that cell calculations were obtained from a one-dimensional transport code and therefore the gross leakage responsible for the low k effective of the system was arbitrarily represented by a transverse leakage. Since the k infinity of STSF cores is normally large (~ 1.67 for STSF-2, ~ 1.30 for STSF-7), the transverse leakage to be used in obtaining a reasonable k effective in a cell calculation was large. However, the transverse leakage in the transport code 1DF is equal to DB^2, where D is the local diffusion coefficient so that the leakage varies strongly from one plate to the other inside the cell. It has therefore not been possible to match the k_{eff} from the calculations of the heterogenous and homogeneous cells. However, the difference in k_{eff} is not accompanied by a difference in the spatial structure of the flux in the cell or in the corresponding disadvantage factors (see Section 5).

Finally, the solution seems to be the use of k_∞ cell calculations for determining absolutely the amplitude of the flux oscillations across the cell. The technique is as follows:

1. Using the first set of cross sections generated by GAM, calculate the space-energy flux in the cell (S_{16}, P_3). Obtain disadvantage factors for k_∞
2. Homogenize the cell, use the second set of cross sections generated with GAM and perform a new S_{16}, P_3, k_∞ calculation. The k_∞ should be identical in both cases if the disadvantage factors have been properly taken into account to shield the cross section of the second set.

For STSF-7, one obtains k_{eff} (heterogeneous) = 1.2957 and k_{∞} (homogeneous) = 1.2979, this is an excellent agreement. It is now possible to obtain an absolute value for the flux heterogeneity by ratioing, for a given position and angle, the result of the heterogeneous calculation to the one of the homogenous calculation.

5. CELL CALCULATIONAL STUDIES

The STSF-2 subcritical assembly consisted of a small, roughly cylindrical core (20.4 cm radius, 22.8 cm half-height) of ^{235}U, ^{238}U, graphite, and Al matrix, surrounded by an inner iron reflector, 18 cm thick, and a depleted-uranium outer reflector, 15 cm thick. Atom densities in the core were 0.00416 atoms/barn-cm for ^{235}U, 0.01054 atoms/barn-cm for ^{238}U, 0.04361 atoms/barn-cm for C, and 0.00564 atoms/barn-cm for Al to give a loading of 95.6 kg ^{235}U. The assembly was excited by a photofission source near the center. Details are given in a previous progress report.[5]

The core had to be represented in the calculations by at least two dimensions because the half-height was nearly equal to radius, because the dimensions were only a few times the average mean-free-path ($\sim$2.5 cm), and because the reflector had a strong influence on the core spectra. The reflected assembly was subcritical (critical mass $\sim$142 kg ^{235}U) and the spectrum changed rapidly near the source (within $\sim$10 cm). The spectrum also changed with radius as the core-reflector interface was approached. Nevertheless, there was an asymptotic region about 10-12 cm from both the interface and the source, where angular-flux spectrum measurements were made and where calculations were desired for comparison with the measurements.

In addition to the complication due to the geometry and to the strong spatial dependence of the spectrum, and probably more serious, was the complication introduced by the heterogeneous distribution of core materials. The core was composed of plates (2 in. by 1/8 in. thick) of enriched uranium (93% ^{235}U), of depleted uranium (99.8% ^{238}U) and graphite, together with the aluminum drawer and structure.

The aluminum is not expected to play a strong role in the spectrum, except at the 36 keV absorption resonance. Most of the aluminum is surrounded by carbon, therefore it should be accurate enough to average the aluminum cross sections over the average spectrum existing in the carbon, (calculated without aluminum present), or since the disadvantage factor for carbon is relatively small, to use unweighted cross sections for aluminum. With the aluminum effectively removed, the repeating unit cell may be chosen as shown in Fig. 5 (other choices are possible, depending on the starting plate, but this choice is reasonable and gives rough symmetry about the centerline). The over-all stacking arrangement was such that the physical unit cell may be considered to extend to eight inches (20.4 cm) in the y-dimension, and 18 inches (45 cm) in the z-direction. However, the leakage effect has to be accounted for by a DB^2 correction in 1DF, with y = z = 37.0 cm according to the prescription reported in Ref. 2.
The time-of-flight spectrum measurements were made by extracting a neutron beam at right angles to the plate, in the x-direction as indicated in the figure, at the surface of the chosen plate.

In order for an S_n calculation to reproduce the fine-structure in the spatial distribution, the mesh has to be rather fine in the x-direction. The true x-y-z dependence could only be reproduced by a three-dimensional code, but a one-dimensional layered slab approximation will give answers accurate enough for our purpose (with suitable adjustments of parameters). Even so, something like 50 mesh points would be desirable and perhaps necessary across the 2.54 cm-wide cell (six per plate). To compute the local as well as the gross spatial dependence of the flux across the whole core in a direct approach would involve 800 mesh points which would be unfeasible, at least if reasonable energy resolution is to be preserved. The heterogeneous structure cannot be ignored however, because previous calculations[2] have shown this structure to lead to significant ($\sim$30% by broad-group) spatial flux variation across the cell and several percent effect on k.

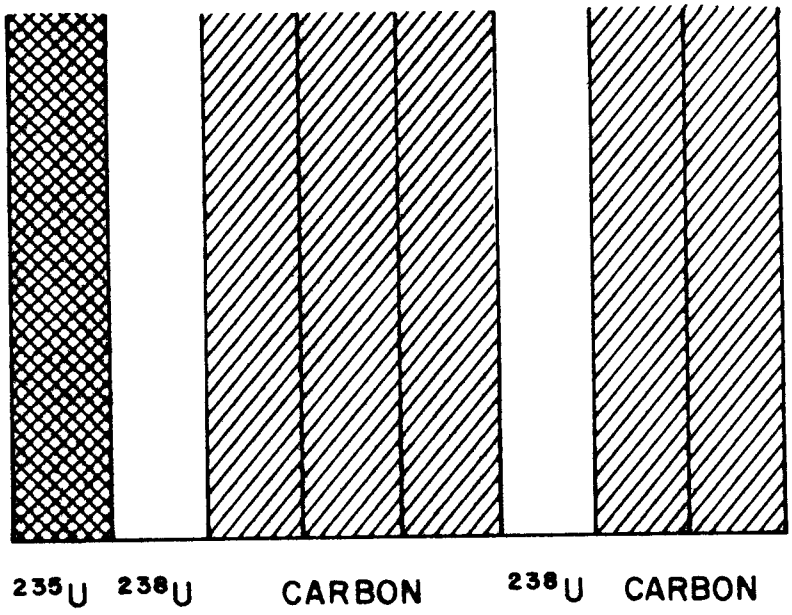

Fig. 5. Repeating unit cell chosen for STSF-2

The existence of a moderately large asymptotic-spectrum region accompanied by the difficulty of representing the geometry adequately suggests attempting to separate the problem into two parts:

1. Calculate the fine-structure within the unit cell with a fine energy mesh, and resonance calculation, and then homogenize the cell into a mixture with broad-group cross sections properly weighted over energy and space.
2. Use the homogenized cross sections to calculate the spatially-dependent flux density spectrum over the core.

If separability holds, we may then combine the fine spatial detail (and possibly energy and angular detail) in: (1) with the over-all spatial dependence, and in (2) to obtain a combined result for comparison with experiment.

The homogenized core cannot be exactly like the heterogeneous core, but may be designed to be equivalent, e. g., in giving the same k_{eff}. The equivalence may preserve over-all reaction rates in the individual plates, or at least near the center, in the spirit of a resonance integral for thermal reactor "resonance escape" calculations. Hopefully, if averaged reaction rates are preserved, k will be calculated accurately once the gross leakage is introduced in the over-all reactor calculation. But matching spectra presents a new complication. Perhaps the best solution is to attempt to calculate spatially-dependent reaction rates and then derive spectra from these. This has not been done in the present work; rather we have attempted to preserve k and hoped the spectrum will follow.

In making the separation into a unit-cell calculation and a gross or over-all calculation, the question arises as to how to handle the influence of the over-all leakage-reflection condition on the energy-space-angle distribution within a "typical" cell. In large thermal reactors, where the unit cell is repeated many times across the radius, and/or where reflection is relatively unimportant (in water reactors), the usual procedure is to perform an infinite-cell calculation. That is, zero-leakage boundary conditions

are imposed. To be specific a "k_∞" calculation is done, with no axial leakage (no DB^2 correction) and periodic boundary conditions in the radial direction of the cell. A 1DF calculation is performed, converging on the fission source (k calculation). It is possible to reiterate the cell calculation, using a fission-source distribution derived from an over-all reactor calculation, but this is usually unnecessary. We have performed such a k_∞ cell calculation and compared the disadvantage factors with a calculation identical except for a DB^2 correction appropriate for the core: this was discussed earlier.

The calculated k_∞ for STSF-2 is 1.682, while k for the finite cell in the core is 0.889. The disadvantage factors, however, are almost the same. The disadvantage factors for the graphite vary from 0.992 at high energy to 1.104 at low energy, and the values from the k_∞ and k calculations agree to better than 1%. The disadvantage factors for the depleted uranium vary from 1.003 to 0.937, and agreement between the values from the two cell calculations is better than 1%. In the enriched uranium, the disadvantage factors vary from 1.064 at high energy to 0.604 at low energy, and the values from the k_∞ and k calculations agree to better than 1% below 1 MeV, and within 2% in the higher-energy groups. The k calculations are higher. Therefore, it appears that a k_∞ cell calculation would be appropriate for disadvantage factors, removing the ambiguity of a DB^2 correction.

6. PROTON RECOIL DETECTOR STUDIES

6. 1 RESPONSE FUNCTION MEASUREMENTS

As it was pointed out in the previous quarterly report, [1] two cylindrical proton recoil detectors were selected for the response function measurements. The characteristics of the two detectors are listed in Table 2. Calibration data obtained from a fit to the Diethorn equation[15] were available for both detectors.

A preliminary experiment was made during the second half of June using the linear accelerator as a neutron source, to determine part of the response function for the two detectors.

A high power, water-cooled uranium target was used to obtain a pulsed neutron beam from the accelerator. The spectrum from this target has been measured previously and is available. [16] The detector under study was positioned at the 100-meter station, the total distance from the target to the center of the detector being 127. 20 meters.

The block diagram of the electronics used during the measurement is illustrated in Fig. 6. Essentially, we have used a two-parameter acquisition system embodying the USAEC owned CDC 1700 computer to measure simultaneously the time-of-flight and the height of the pulses from the detector.

When using proton recoil chambers, a major problem is encountered from gamma rays which can give ionization pulses comparable to the neutron pulses. A well known way of distinguishing neutron from gamma pulses is the technique of pulse shape discrimination[17] which is based on the fact that the neutron pulses have a faster rise time than the pulses originating from gammas giving the same ionization.

Table 2

DETECTOR SPECIFICATIONS

	Hydrogen Detector	Methane Detector
Over-all Diameter	1-1/2 in.	1-1/2 in.
Body Length	5-1/2 in.	5-1/2 in.
Effective Length	3 in.	3 in.
Anode Diameter	0.001 in.	0.001 in.
Gas Filling	200 cm (Hg) Hydrogen 10 cm (Hg) Methane 10 cm (Hg) Nitrogen	258 cm (Hg) Methane 12 cm (Hg) Nitrogen

Therefore, the ideal way of measuring neutron response functions is to record simultaneously the height of the pulse V, the time-of-flight t and the derivative dV/dt. Since a computer code for the CDC 1700 to do this type of collection was not initially available, we used a two-parameter code. However, we looked also at dV/dt during the measurement, by using a TMC analyzer and an energy window set by an external discrimination.

One measurement was made with the hydrogen detector at 3000 volts and the detector parallel to the flight path. Two measurements were made using the methane detector at 3000 volts, in both parallel and normal positions.

The high voltage, discrimination level and time gate were set so that the hydrogen detector provided information for ionizations between 10 keV and 100 keV while the methane detector provided information for ionizations between 300 keV and 1000 keV. For the hydrogen chamber, the TMC analyzer recorded dV/dt between 58 keV and 71 keV, while for the methane detector this window was set between 760 keV and 840 keV. For both of these ranges of ionization we observed only one peak in dV/dt, corresponding to the position of the neutron peak as observed with a 10 curie PuBe source.

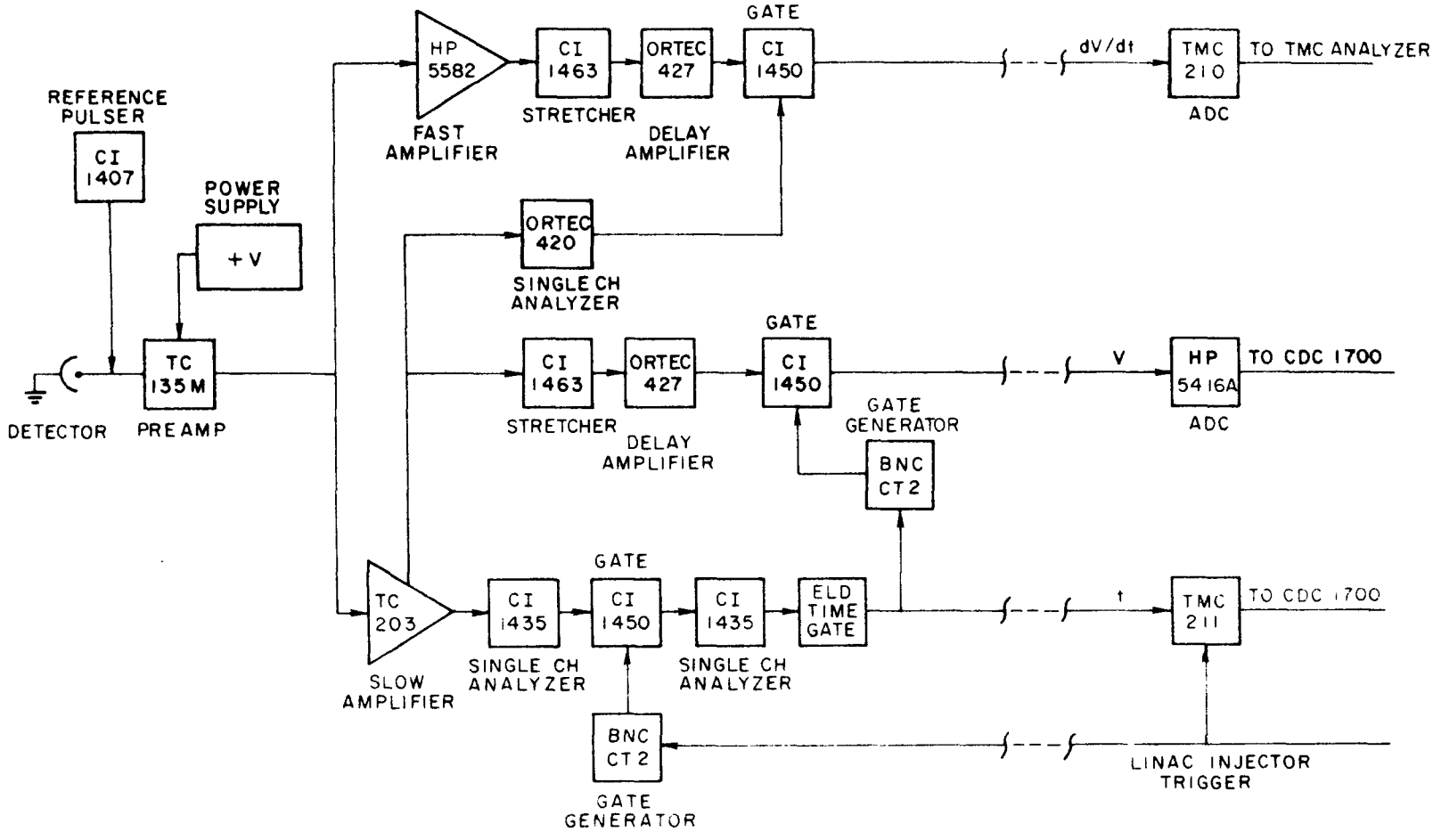

Fig. 6. Electronics block diagram for response function measurements

Before the experiment the energy scale was calibrated by exposing the chambers to thermal neutrons and using the $^{14}N(n, p)C^{14}$ reaction, caused by the small amount of nitrogen gas contained in the chambers.

Figure 7 shows the nitrogen line for the H_2 detector and gives an idea of the detector resolution.

The gamma background was measured with a 7-in. polyethylene filter between the target and the detector. The polyethylene filter scatters practically all the neutrons out of the flight path, slightly reducing the intensity of the transmitted gammas. The background counting rate was found to be extremely small, about 0.76% of the total counting rate and therefore a very long run would have been necessary to acquire meaningful statistics. For this reason a detailed background measurement was not made.

The data were analyzed by sorting the two-parameter data. This analysis has not been completed yet but some examples are given. Figure 8 shows the response function for the hydrogen detector at energies between 50 keV and 60 keV. Figure 9 shows the response function for the CH_4 detector at energies between 300 keV and 375 keV. Similarly, Fig. 10 shows the response function for the CH_4 detector between 850 and 900 keV. It is too early to speculate on the significance of these data. However, a preliminary look at the measured response functions shows that they are in qualitative agreement with measurements performed under a different project[18] on a larger CH_4 detector.

6.2 ANALYTICAL STUDIES

Work has begun on the coding of equations which compute the wall and end effects for cylindrical counters. The equations were first derived by Snidow and Warren[19] and provide an analytical description of the response function for cylindrical detectors. Presently, we have a Monte Carlo type code (WEND) which can compute response functions for a neutron beam parallel to the detector axis.

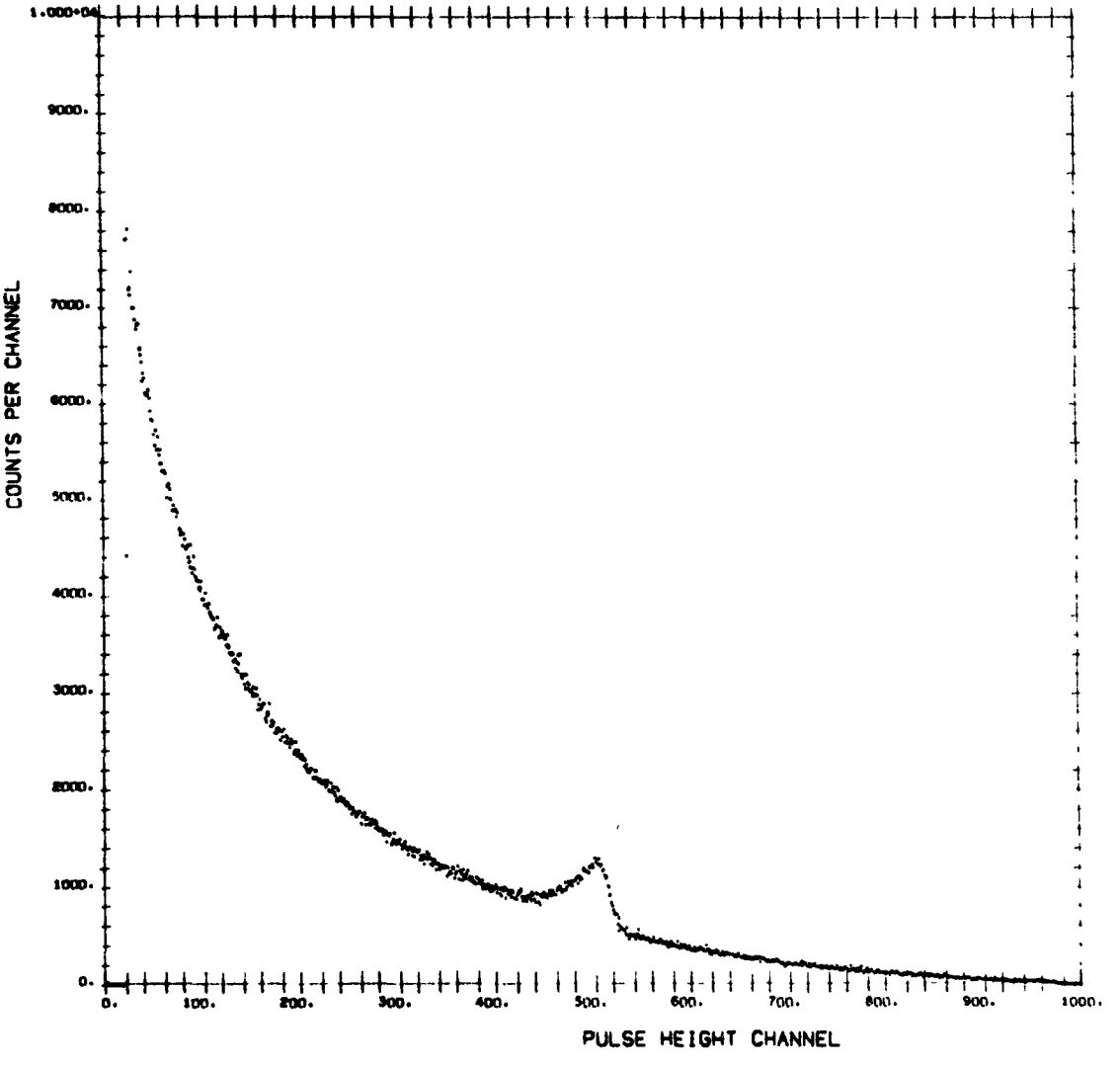

Fig. 7. Energy calibration from N_2 line for the H_2 detector

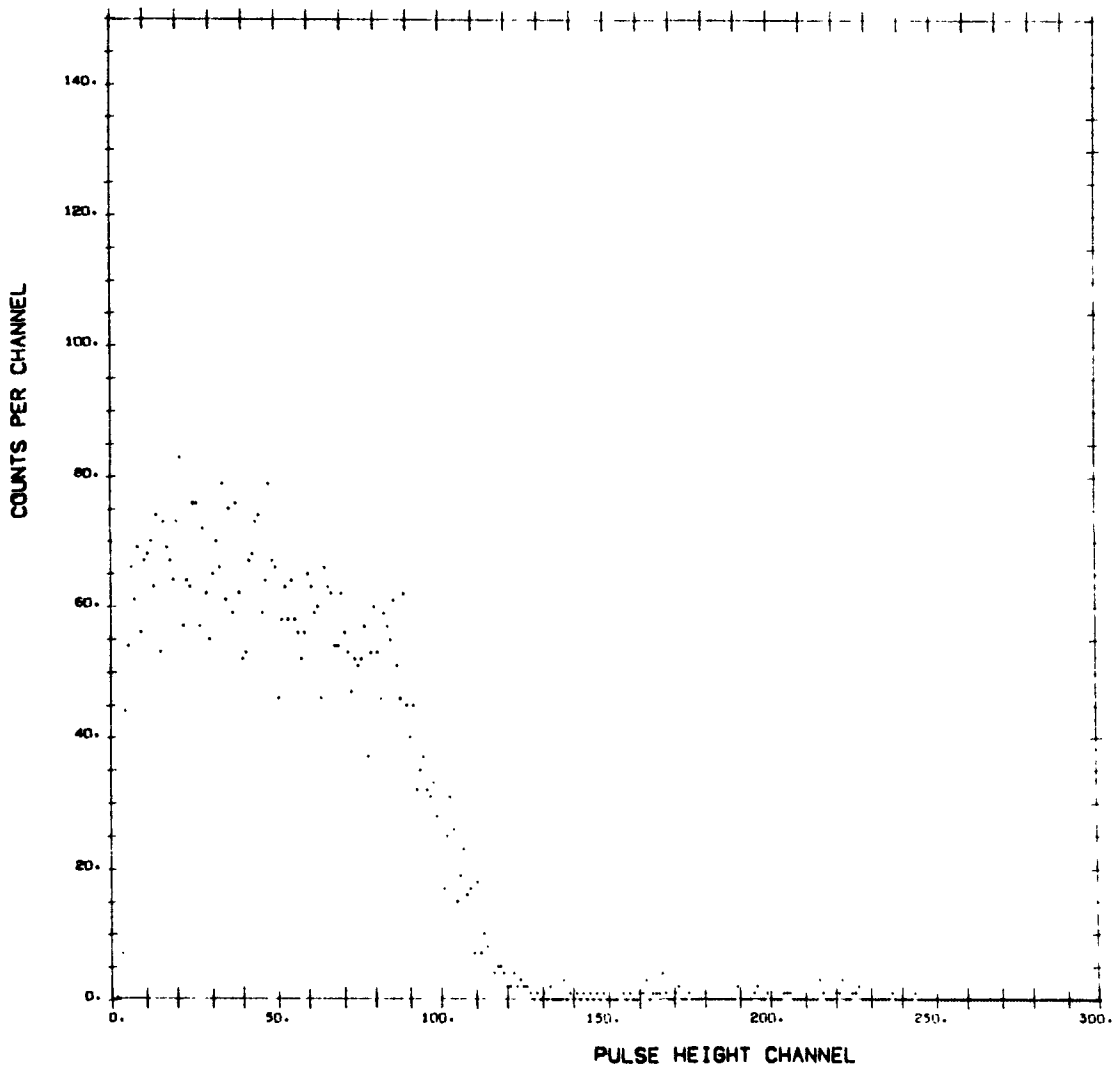

Fig. 8. Response functions for the H_2 detector parallel to the beam. Range: 50 keV – 60 keV.

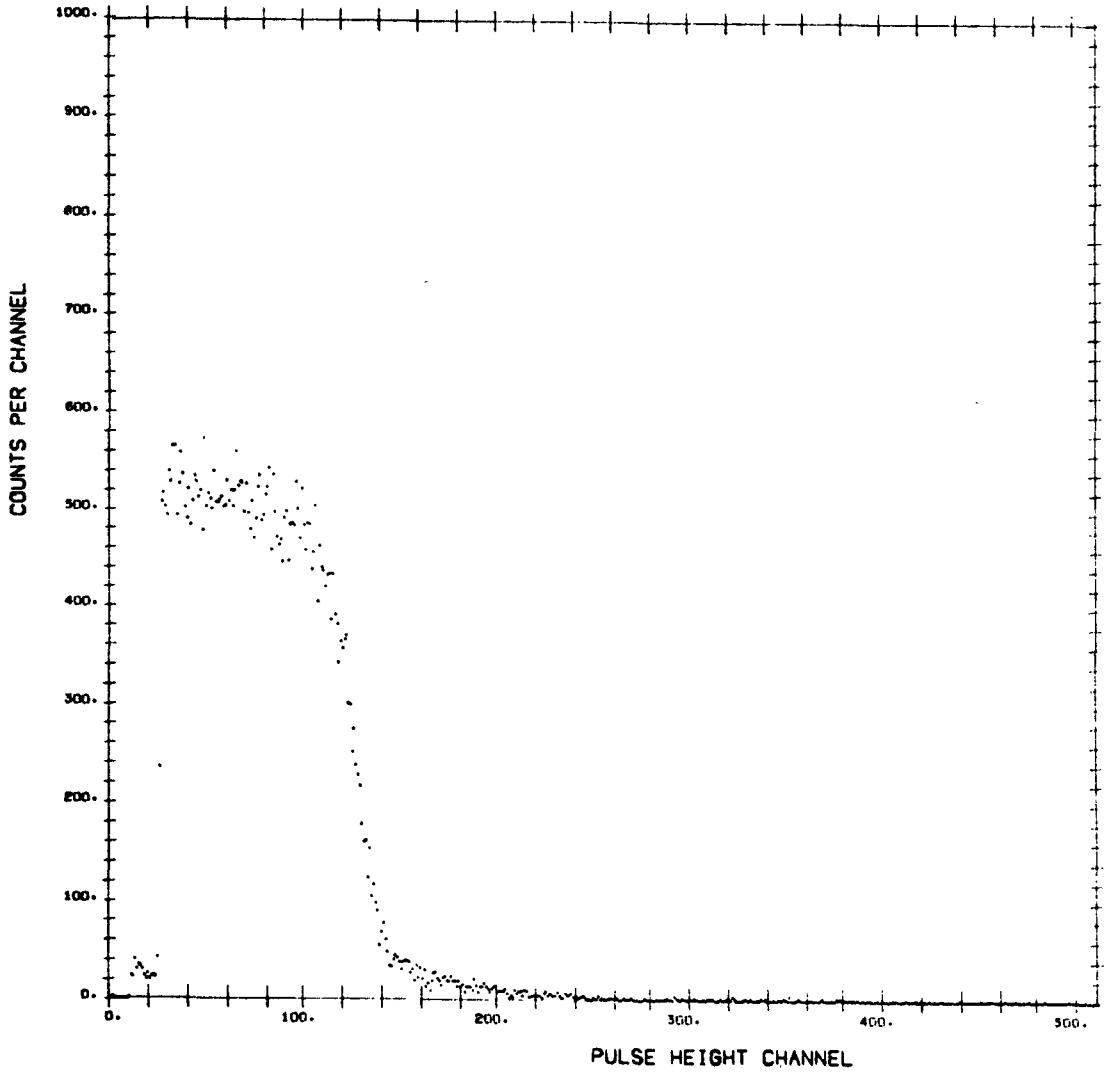

Fig. 9. Response function for the CH_4 detector parallel to the beam. Range: 300 keV – 325 keV.

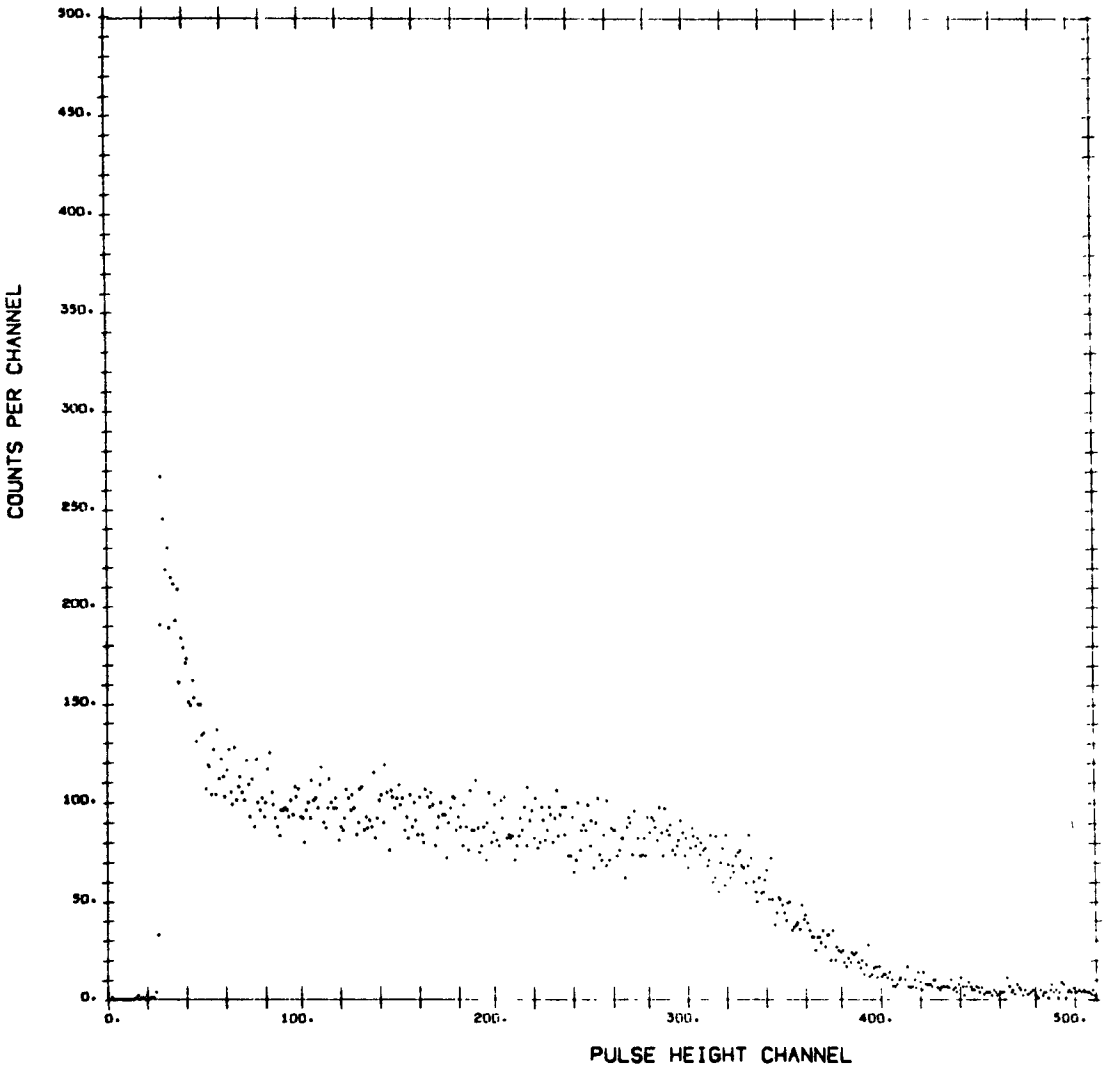

Fig. 10. Response function for the CH_4 detector parallel to the beam. Range: 850 keV – 900 keV.

6.3 THREE-PARAMETER CODE FOR CDC-1700

While the measurements seemed to indicate that the gamma contribution in the measurement of the response function is a minimum, at least in the energy range observed, still there is no guarantee that the same situation will hold at higher energies. Therefore, it was decided to go ahead and write a three-parameter data acquisition code for the CDC-1700 computer. The code has now been written and will be used in the next measurement of the response functions.

The code reads digital numbers from three analog-to-digital converters that can be selected arbitrarily by the user. These three numbers are written on the disk and they are also used to increment some banks of locations in core. The program allows for one bank of 1000 channels for time, one bank of 1000 channels for pulse height, V, and three banks of 64 channels for dV/dt corresponding to three selectable values of ionization. All these banks are displayed on the scope so that it will be possible to monitor the data during the experiments.

To save space on the disk, V and dV/dt are written on it as a single 16-bit word of the CDC-1700. This is obtained by reserving 10 bits for the V information and 6 bits for the dV/dt information.

The code has all the standard features of the previous two-parameter code and it will allow for typing the information in core on the teletype, resetting, writing the information in core on disk banks (different than the ones where the raw data are stored) and indicating the position on the disk at which the raw data are being stored.

6.4 NEUTRON SPECTRUM MEASUREMENTS IN STSF-7

After the final loading of STSF-7 was completed, the hydrogen and the methane proton recoil chambers were used for measuring the spectrum of the reactor. Each detector, which is 1.5 inches in diameter, was placed in a cylindrical hole in a 2 in. x 2 in. x 4 in. lead block meant to reduce

the gamma flux in the detector. The lead block was then placed inside a standard aluminum drawer, with the signal cable running along the drawer and going to the preamplifier located just outside the assembly. The space around the cable was filled with ^{238}U to reproduce as much as possible the original configuration of the reactor and thus to minimize the perturbations introduced by the detector system.

Measurements were performed with the two detectors both in the core and in the reflector. When the detectors were in the core (position M14) a 1-curie PuBe source was used as the neutron source, while with the detectors in the reflector (position M19) a 10-curie PuBe source was used. With this arrangement the counting rates in the two situations were of the same order of magnitude.

Pulse shape discrimination was used for the lower range of ionizations. The electronics block diagram for pulse shape discrimination is shown in Fig. 11. This arrangement was used previously and is described in Ref. 20.

The hydrogen detector was used at high voltages of 2400, 2800, 3000, 3200, 3400, and 3600 volts, both in the core and in the reflector. The measurements at 3400 volts was done with a TMC analyzer (conventional pulse height measurement) while all the others were done with both the TMC analyzer and the CDC-1700 computer in a two-parameter accumulation mode.

The methane detector was used at high voltages of 3000, 3200, 3400, and 3600 volts, both in the core and in the reflector. The measurements of 3000 and 3200 volts were done with the TMC analyzer while the others were done with both the TMC and the computer. A total of 39 runs, including calibrations, were performed.

The information collected has not been analyzed yet, but work has begun in the coding of a numerical algorithm for the analysis of the pulse shape discrimination data.

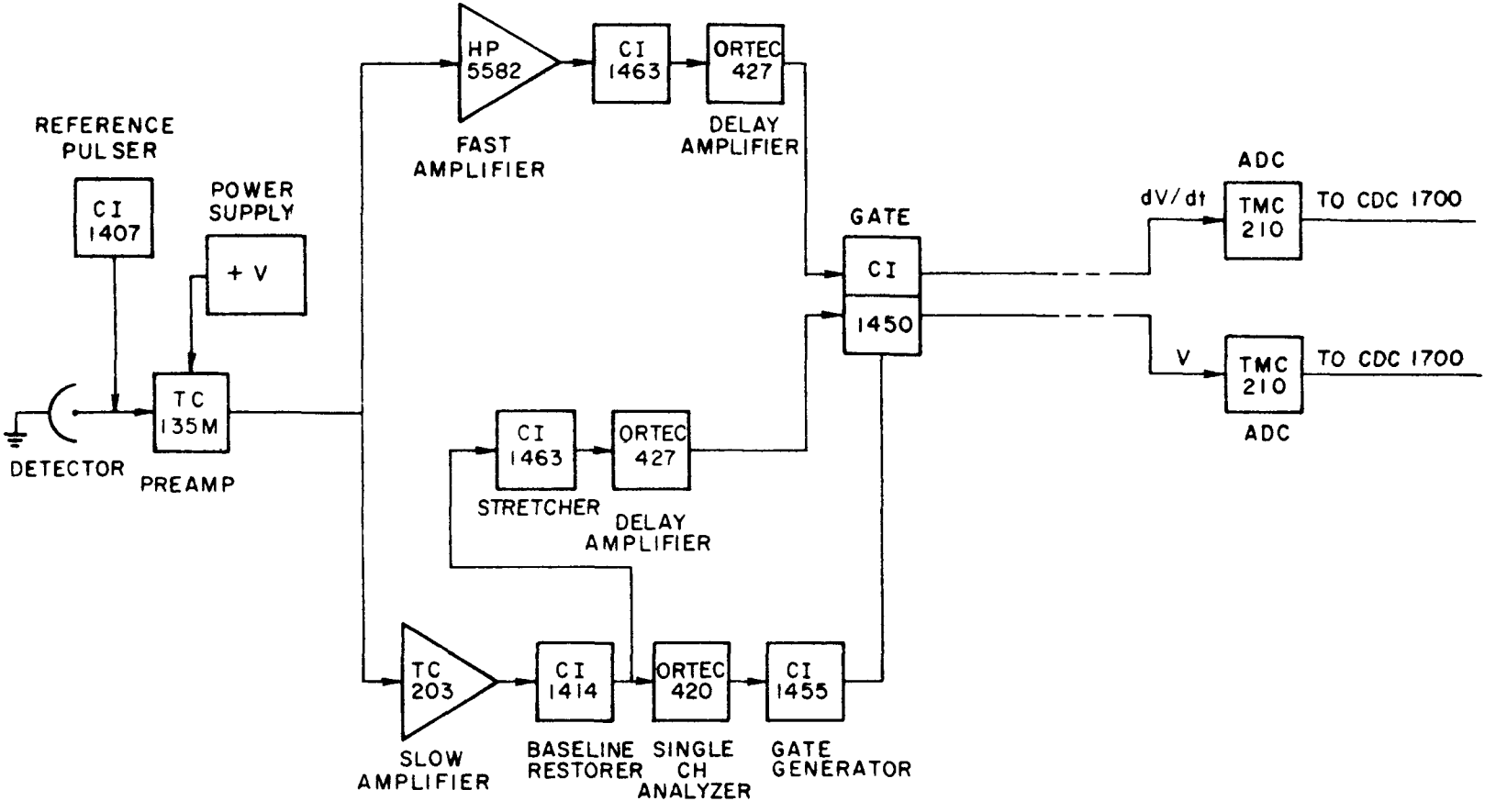

Fig. 11. Electronics block diagram for reactor spectrum measurements

The two-parameter pulse shape discrimination program for the CDC-1700 stores all the data in the core in the form of dV/dt in 128 banks of 64 channels each. Usually the content of one of these banks consists of two peaks, one given by the gammas and one given by the neutrons. The information of interest is the area of the neutron peak and therefore some way of extracting this information from the data is needed.

Previously the subtraction of the gamma contribution was done by hand, after fitting by eye the decaying gamma curve. This work would be exceedingly time consuming and therefore we have decided to use the computer and obtain an analytic fit to the data. We are presently trying to fit the neutron peak with a gaussian and the gamma peak with an asymmetric gaussian. After the fit, the area of the neutron peak can easily be obtained by subtracting the gamma contribution from the data.

Figure 12 shows some typical data together with a preliminary fit. The continuous curve is the analytic fit to the data. The neutron and gamma components are also shown.

Since it may be dangerous to rely entirely on a computer analysis of the data (a bad channel can alter substantially the quality of the fit) we are also planning to use the plotter to obtain for all the data analyzed a plot of the data and the corresponding fit. Due to the large amount of data collected, a way to conveniently compress the plotting format will have to be devised.

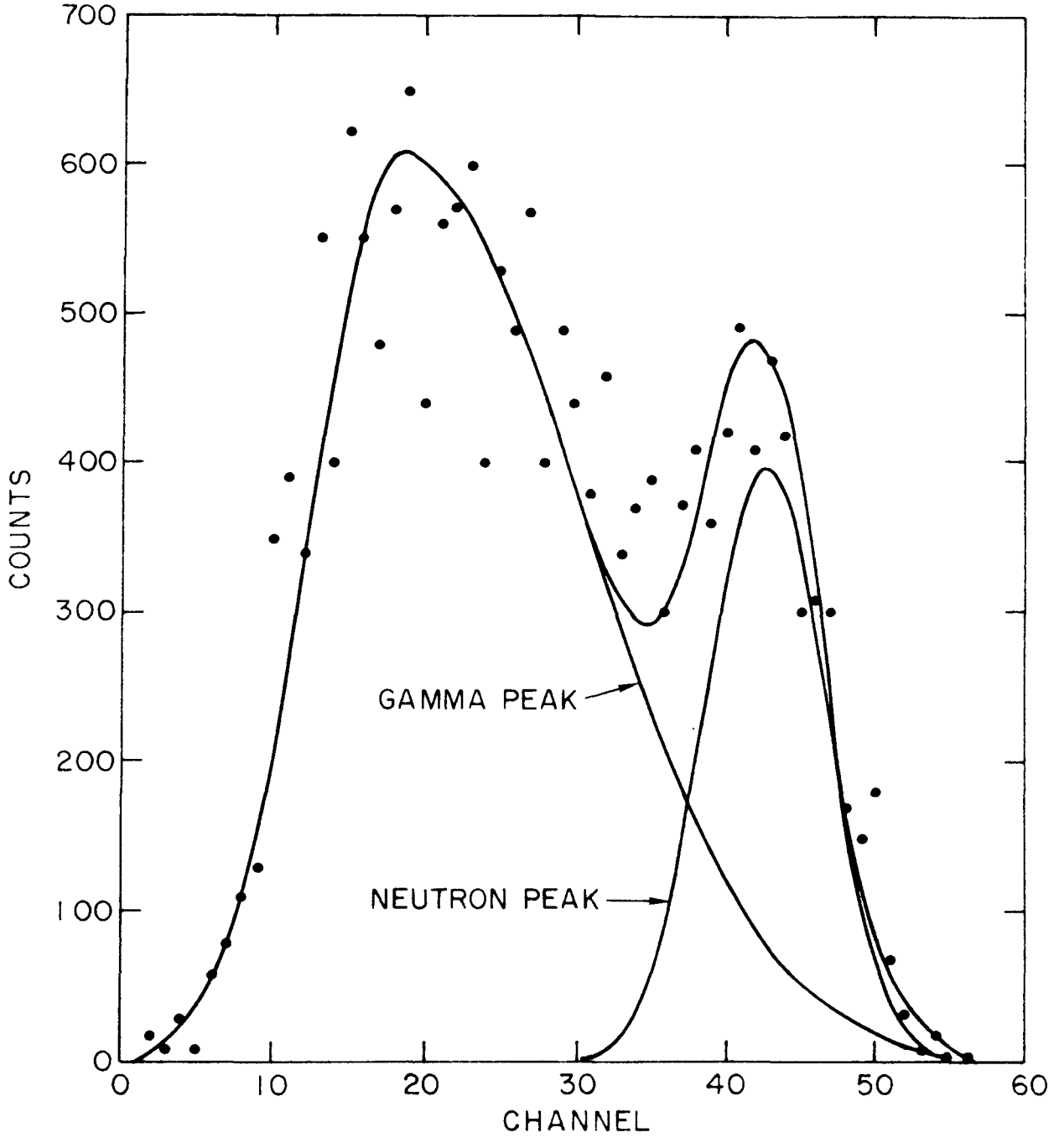

Fig. 12. Typical pulse shape discrimination data and fit

7. ^{3}He NEUTRON SPECTROMETER

The ORTEC type 525 ^{3}He neutron spectrometer has been put into operation.

The principle on which this spectrometer is based is well known: two 2.5 cm^2 surface barrier silicon detectors mounted face to face 1 mm apart define a 0.25 cm^3 volume filled with ^{3}He gas. When a n(^{3}He, T)p reaction takes place inside that volume, the proton is stopped by one detector and the triton by the other. The total energy deposited in the two detectors is equal to the neutron energy E_n plus 764 keV (the reaction Q value)

$$n + {}^3He \rightarrow p + T + 764\ keV\ .$$

The main purpose for the acquisition of this detector is the measurement of the time-energy response of STSF when the assembly is pulsed by the Linac for neutron spectrum measurements by time of flight. Accurate neutron emission time corrections are indeed required for the reduction of such spectra. The ^{3}He spectrometer is, in principle, a good way to measure such responses. The relative energy resolution of the spectrometer is about 100% at 100 keV, 25% at 500 keV, and 15% at 1 MeV.

Figure 13 is a block diagram of the electronic setup associated with the spectrometer. Figure 14 shows typical results obtained with a thermal neutron source; they compare favorably with recent results reported by other laboratories.[21, 22] The next steps to be taken in the use of the detector are:

1. Measure the steady-state spectrum of STSF-7 so as to make possible a comparison with proton recoil detectors and time-of-flight measurements.

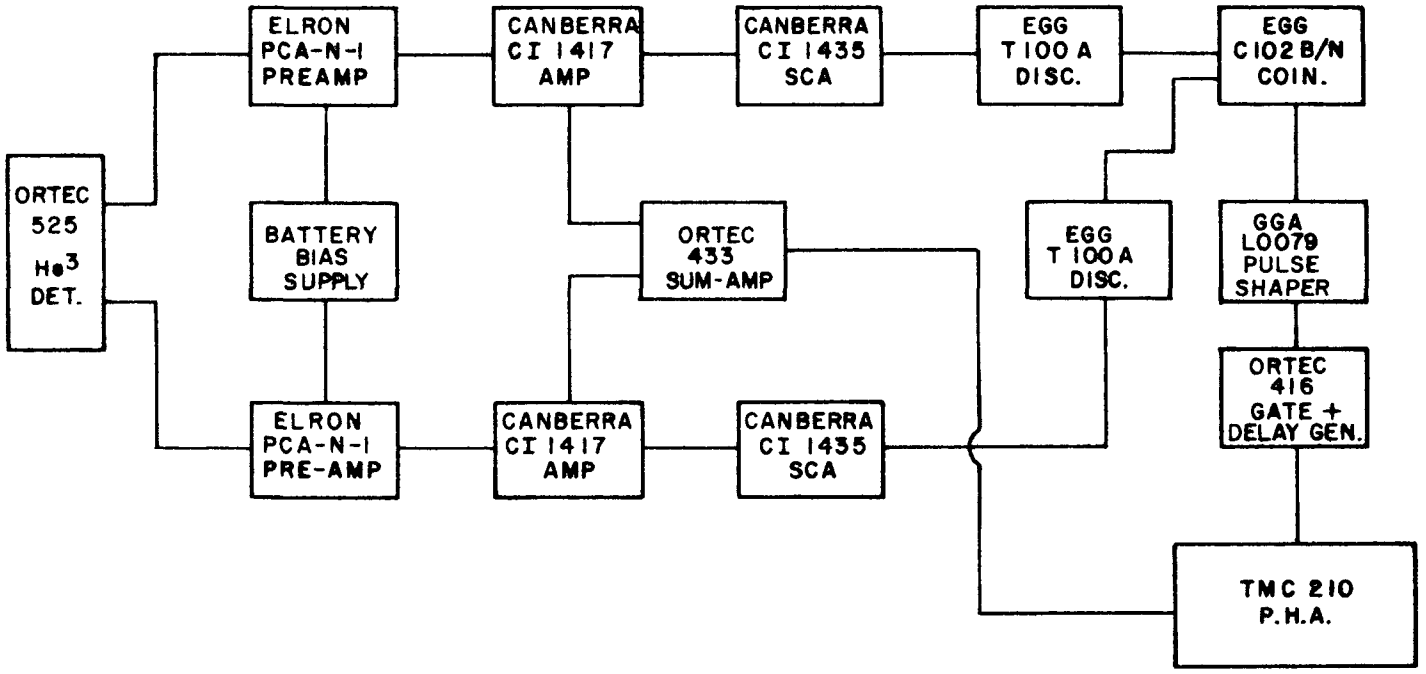

Fig. 13. Block diagram for ^{3}He neutron spectrometer

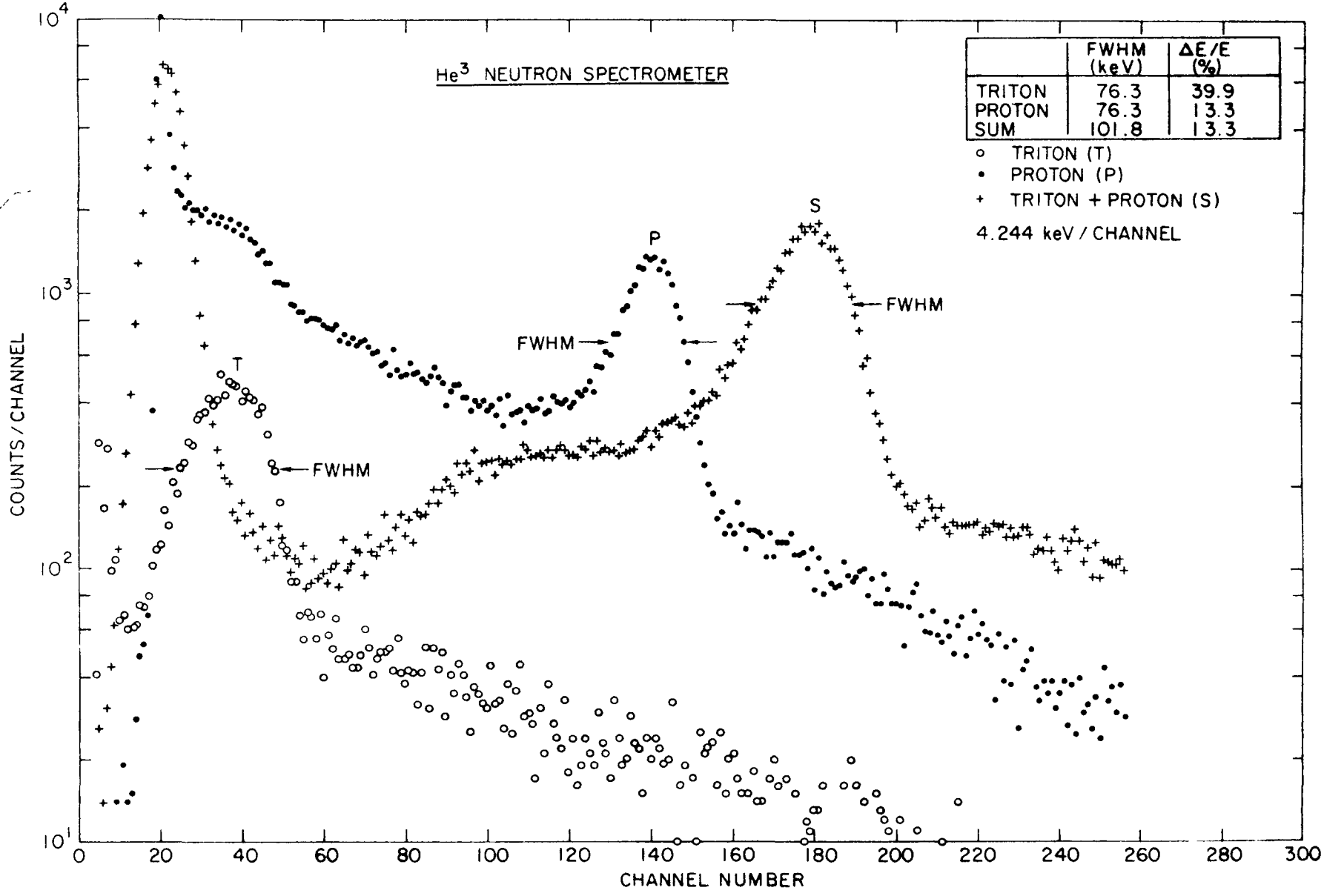

Fig. 14. Data showing the proton, triton and sum peak from ^{3}He detector

2. Compare the energy integrated time-dependent response of the detector with the one from a ^{10}B chamber during pulsed neutron experiments in STSF-7.

Finally, if these two tests are satisfactory, measurements of the time-energy neutron flux in an assembly will be made.

As a final remark, let us point out that, even though the efficiency of the detector can be calculated rather accurately below 2 MeV, it would be desirable to obtain experimental information about this efficiency. This can probably be done by measuring a known spectrum; the ^{252}Cf fission spectrum would be adequate.

8. TIME-DEPENDENT ANISN CODE

The major effort on the time-dependent ANISN Code (TDA)[23] has been its conversion to the UNIVAC 1108. The results of some test problems are presented below.

The first problem is that of a uniform semi-infinite slab with a step function first collision source, $S\delta(x)\,\delta(\mu = 1)$. The parameters of the problem are:

	Group 1	Group 2
Velocity	1×10^8 cm/sec	5×10^7 cm/sec
Collision Source Density	1	0
$\Sigma_{absorption}$	2.0 cm^{-1}	3.0 cm^{-1}
Σ_{total}	10.0 cm^{-1}	15.0 cm^{-1}
$\Sigma_{self\ scattering}$	2.667 cm^{-1}	12.0 cm^{-1}
$\Sigma_{down\ scattering}$	5.333 cm^{-1}	—

The geometry is a slab, 2 cm thick, with vacuum boundary conditions, and the source is normally incident at x = 0, with a burst duration of 10^{-11} sec. The flux vs position at a given time for group 1 is shown in Fig. 15.

The second problem has a uniform step function source S of 10^{-11} sec duration. This is a slab problem whose dimensions are the same as the first problem except that the boundary conditions are now reflective. This was done to approximate an infinite medium. The parameters of this problem are:

	Group 1	Group 2
Velocity	1.0×10^{8} cm/sec	2.5×10^{7} cm/sec
Source Density	1	0
$\Sigma_{absorption}$	$2.0\ cm^{-1}$	$3.0\ cm^{-1}$
Σ_{total}	$10.0\ cm^{-1}$	$15.0\ cm^{-1}$
$\Sigma_{self\ scattering}$	$2.667\ cm^{-1}$	$12.0\ cm^{-1}$
$\Sigma_{down\ scattering}$	$5.333\ cm^{-1}$	—

An analytical solution can also be calculated for this problem. Using the above parameters the solution is:

$$\text{Group 1: } \varphi_1(t) = 1 \times 10^{-3}\, e^{-7.33 \times 10^{8} t}$$

$$\text{Group 2: } \varphi_2(t) = 2.9 \times 10^{-4} \left(e^{-0.75 \times 10^{8} t} - e^{-7.33 \times 10^{8} t}\right) .$$

The results of both the analytic and TDA calculations are presented in Fig. 16. During the time shown, both the analytic and TDA agree for Group 2, but the decay is different for Group 1. This problem has not been resolved. It may be that the approximation of an infinite slab by a finite one with reflective boundary conditions is incorrect.

Test problem three, a multiplying system, has been formulated by Zolotar at Argonne National Laboratory.[24] Our results agree with his within the prescribed accuracy. The parameters are:

	Group 1	Group 2
Velocity	1.0×10^{8} cm/sec	2.2×10^{5} cm/sec
Source	1	0
Fission Spectrum	1	0
$\Sigma_{absorption}$	$1.38 \times 10^{-2}\ cm^{-1}$	$2.61 \times 10^{-1}\ cm^{-1}$
$\nu\Sigma_{fission}$	$1.95 \times 10^{-2}\ cm^{-1}$	$4.98 \times 10^{-1}\ cm^{-1}$
Σ_{total}	$1.97 \times 10^{-1}\ cm^{-1}$	$8.14 \times 10^{-1}\ cm^{-1}$
$\Sigma_{self\ scattering}$	$1.66 \times 10^{-1}\ cm^{-1}$	$5.52 \times 10^{-1}\ cm^{-1}$
$\Sigma_{down\ scattering}$	$1.64 \times 10^{-2}\ cm^{-1}$	—

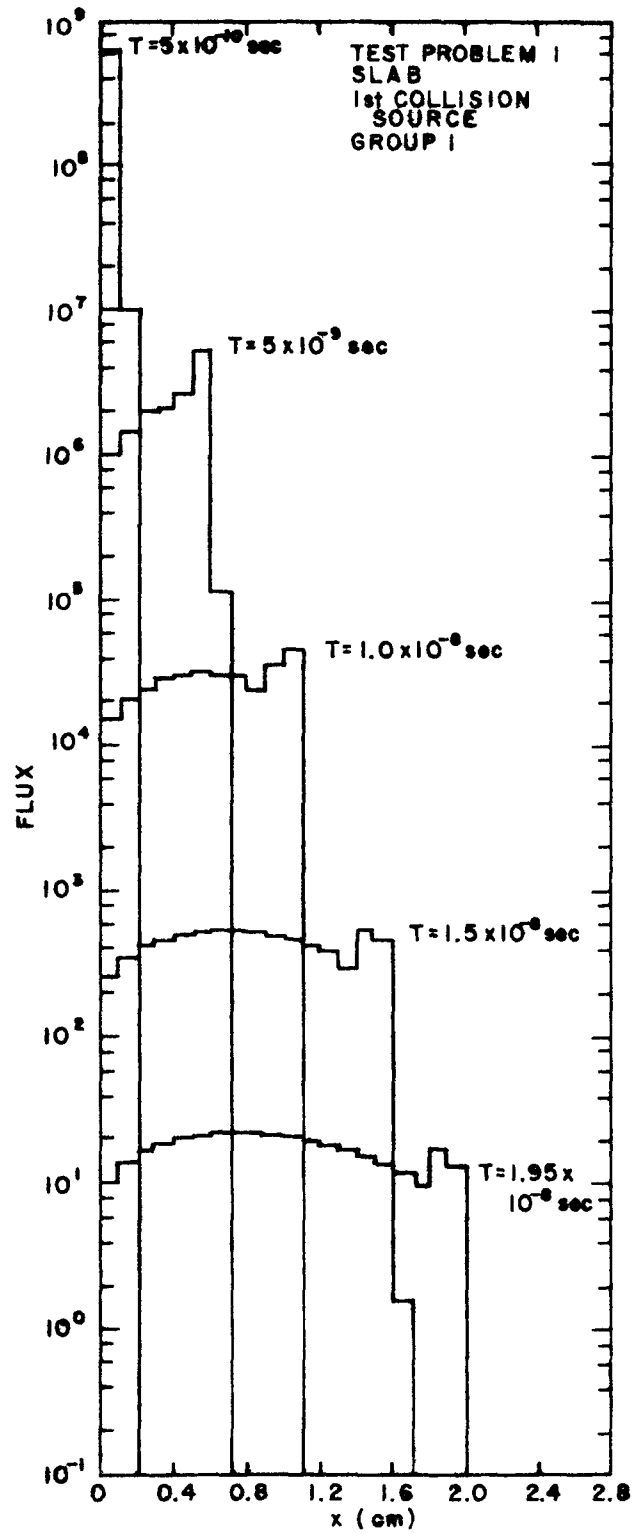

Fig. 15. Flux vs. position for several times for Group 1 resulting from test problem 1

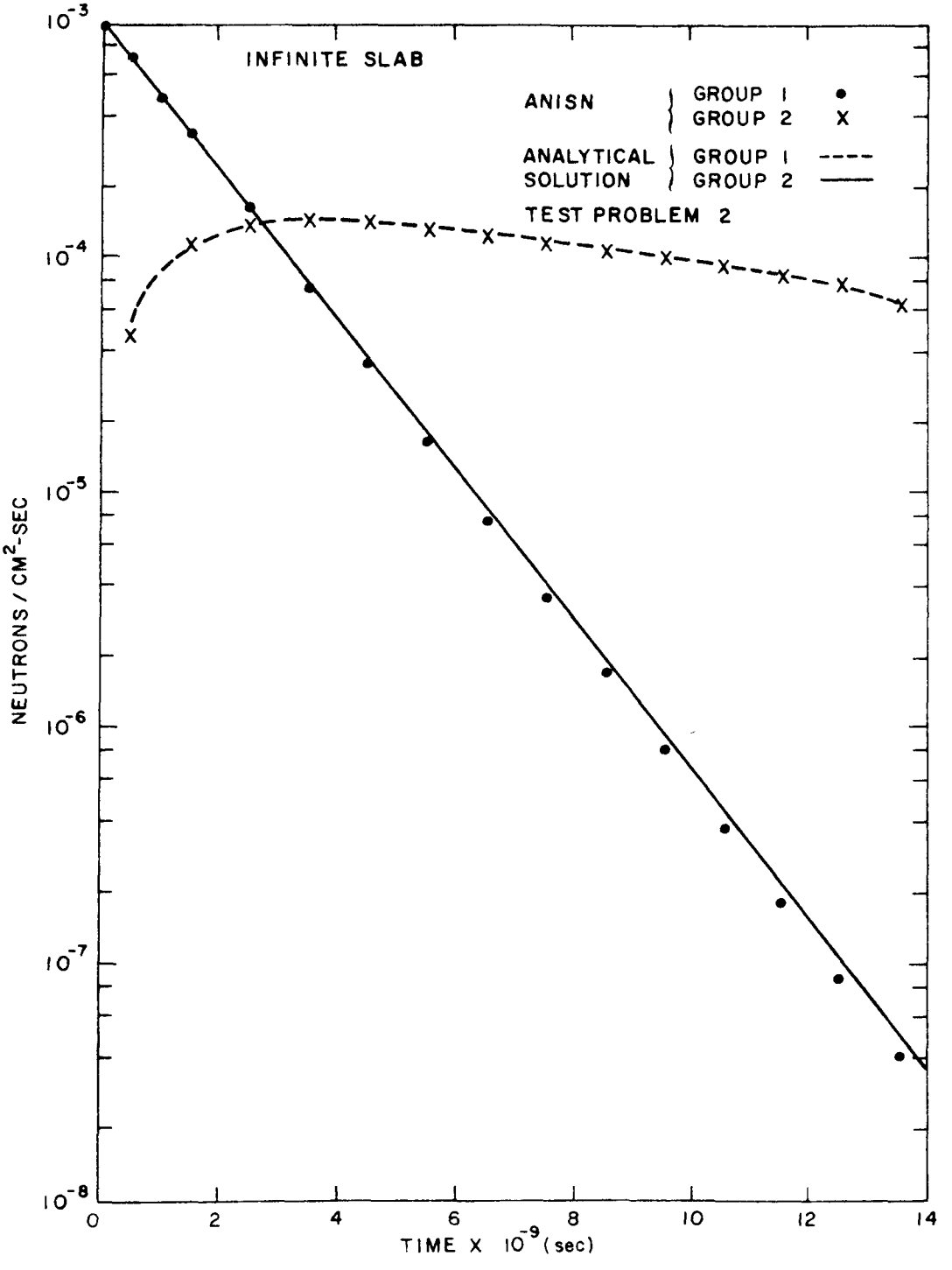

Fig. 16. Results of TDA and analytical calculations for test problem 2

The geometry is spherical with reflective boundary conditions at the center and vacuum at the surface and, the step function source is for 10^{-8} seconds. The fluxes J for groups one and two, at long times, and at the center of the sphere are presented in Fig. 17. A static solution was obtained at Argonne using an α/v search. This gave an $\alpha = -1.272 \times 10^{4}$ secs^{-1}. Our calculation gave an $\alpha = -1.18 \times 10^{4}$ secs^{-1}.

In general, the results of these test cases are very promising. Further tests are planned, for example the calculation of the depleted uranium sphere,[25] for which the TDA calculation can be compared with experimental results. The differences between the analytical and TDA results in problem 2 must be reconciled, and problems with upscattering should be run.

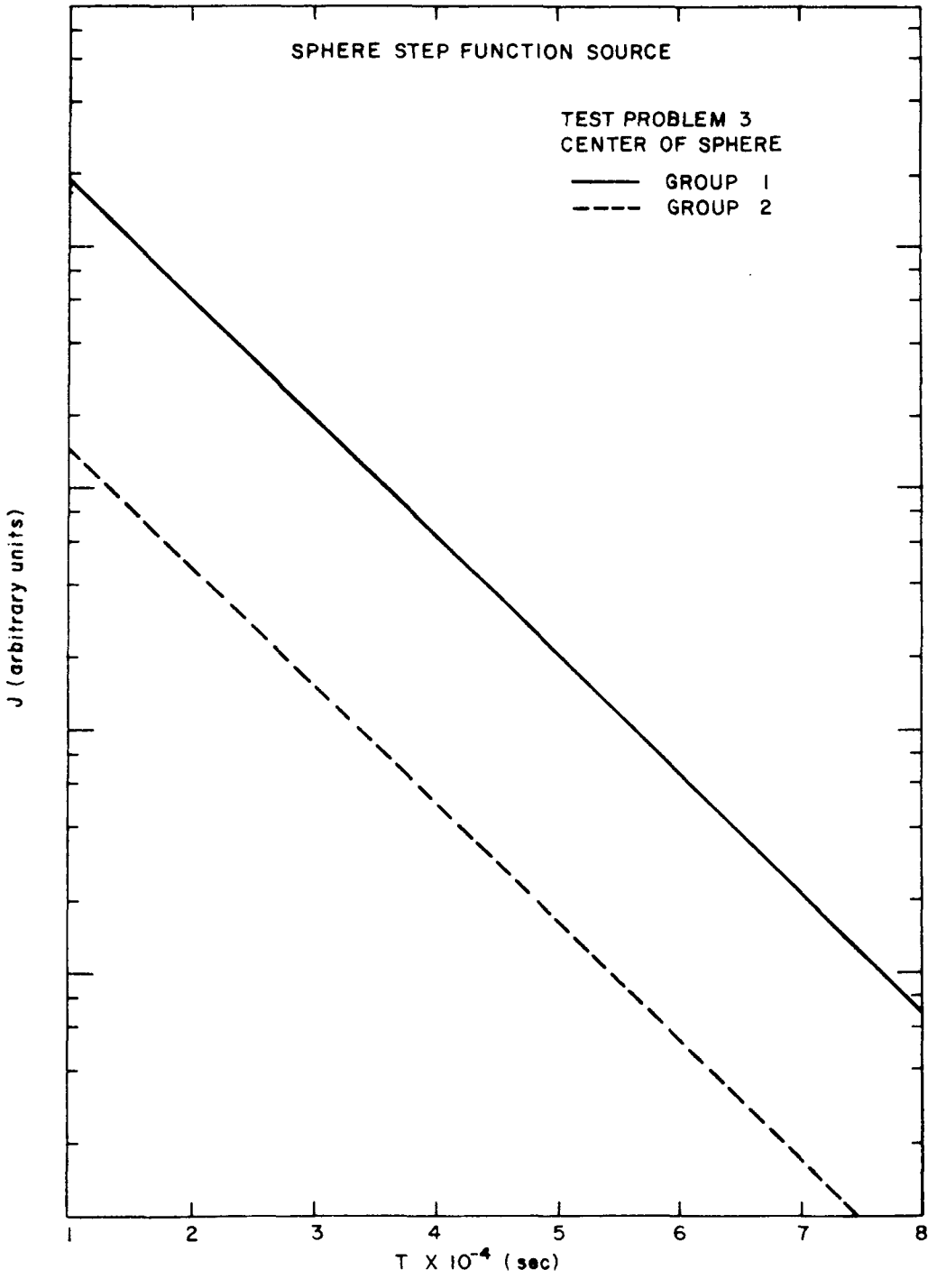

Fig. 17. Results of calculations for test problem 3

REFERENCES

1. J. C. Young, P. d'Oultremont, J. M. Neill, G. M. Borgonovi, D. H. Houston, "Fast Reactor Spectra Measurements," USAEC Report GA-10146, Gulf General Atomic Incorporated, May 15, 1970.

2. J. C. Young, P. d'Oultremont, J. M. Neill, "Fast Reactor Spectrum Measurements – Technical Summary Report," USAEC Report GA-9946, Gulf General Atomic Incorporated, February 27, 1970.

3. J. C. Young, P. d'Oultremont, J. M. Neill, "Fast Reactor Spectrum Measurements," USAEC Report GA-9818, Gulf General Atomic Incorporated, November 13, 1969.

4. J. C. Young, P. d'Oultremont, C. E. Creutz, J. M. Neill, "Fast Reactor Spectrum Measurements," USAEC Report GA-9669, Gulf General Atomic Incorporated, August 15, 1969.

5. J. C. Young, P. d'Oultremont, R. J. Cerbone, J. M. Neill, "Fast Reactor Spectrum Measurements," USAEC Report GA-9386, Gulf General Atomic Incorporated, May 15, 1969.

6. C. A. Preskitt, P. d'Oultremont, J. C. Young, J. M. Neill, "Fast Reactor Spectrum Measurement," USAEC Report GA-9259, Gulf General Atomic Incorporated, March 28, 1969.

7. C. A. Preskitt, J. M. Neill, and J. C. Young, "Fast Reactor Spectrum Measurements," USAEC Report GA-8715, Gulf General Atomic Incorporated, June 3, 1968.

8. J. K. Long, et al., Proceedings of the Second U. N. Conf. on the Peaceful Use of Atomic Energy, Vol. 12, 1958, p. 119-141.

9. "Argonne National Laboratory, Reactor Physics Division Annual Report, July 1, 1968 to June 30, 1969," ANL-7610, January 1970.

10. J. Adir and K. D. Lathrop, "Theory and Method Used in the GGC-4 Multigroup Cross Section Code," Gulf General Atomic Report GA-9021, October 1968. (GAM in the fast neutron section of GGC-4.)

11. K. D. Lathrop, "DTF-IV Code, a FORTRAN-IV Program for Solving the Multigroup Transport Equation with Anisotropic Scattering," USAEC Report LA-3373, Los Alamos Scientific Laboratory, July 1965. (1DF is a Gulf General Atomic modification of this code.)

12. W. G. Davey, "k Calculations for 22 ZPR-III Fast Reactor Assemblies Using ANL Cross Section Set 635," ANL-6570, May 1962.

13. J. M. Kallfelz, B. A. Zolotar and B. R. Sehgal, "Modifications to Fissile Element Cross Sections and Their Influence on Calculated Fast Reactor Parameters," ANL-7610, Section II-32, p. 224, January 1970.

14. A. Hess, ANL Transactions, Private Communications.

15. W. Diethorn, "A Methane Proportional Counter System for Natural Radio-Carbon Measurements," NYO-6628 (1956).

16. S. J. Friesenhahn, et. al., "Annual Summary Report Neutron Capture Cross Sections of Molybdenum, Tantalum, ^{238}U," NASA Report GA-10194, Gulf General Atomic Incorporated, 1970.

17. E. F. Bennett, "Neutron Spectrum Measurements in a Fast Critical Assembly," Nucl. Sci. Eng., 27, 28 (1967).

18. W. M. Lopez, et. al., "Neutron Capture Cross Sections of Tungsten and Rhenium," NASA Report CR-72474, Gulf General Atomic (1968).

19. N. L. Snidow and H. D. Warren, "Wall Effect Corrections in Proportional Counter Spectrometers," Nucl. Inst. and Methods, 51, 109 (1967).

20. R. J. Harris, Jr., "Neutron Spectrum Measurements in Liquid Nitrogen," GA-9886 (1969).

21. T. R. Jeter and M. C. Kennison, "Recent Improvements in He^3 Solid State Neutron Spectrometry," IEEE Transactions on Nuclear Science, February 1967.

22. Itsuro Kimura, Shu A. Hayashi, Katsuhei Kobayashi, Shinji Ishihara and Toshikazu Shibata, "Measurement of Fast Neutron Spectrum with ^6Li and ^3He Sandwich Counters," KURRI-TR-67, Research Reactor Institute, Kyoto University, Kumatori, Sennan-gun Osaka-fu, Japan.

23. W. Engle, ORNL, Private Communication.

24. B. Zolotar, ANL, Private Communication.

25. T. Gozani, "Experimental Neutron Kinetic Studies in a ^{238}U Sphere," Nucl. Sci. & Eng. 36, 143-158 (1969).